Modeling and control of a DC upset resistance butt welding process

Proceedings of the 2007 American Control Conference
Marriott Marquis Hotel at Times Square
New York City, USA, July 11-13, 2007

Modeling and Control of a DC Upset Resistance Butt Welding Process

Gerrit Naus[1], Rudolf Meulenberg[2], René van de Molengraft[1]

Abstract— **This paper presents the analysis and synthesis of modeling and control of the DC upset resistance butt welding process used in rim production lines. A new control strategy is developed, enabling active control of the welding seam temperature and the upset size. As a result, set-up times and energy consumption are reduced significantly.**

I. Introduction

Various types of wheel rim production lines can be distinguished. This distinction mainly lies in the production of the basis cylinder in the so-called preparation line. A widespread and relatively simple production method is based on the coiling of sheets of metal, which are then welded together with an Upset Resistance butt Welding (URW) process: after cutting-to-length sheets of metal, the sheets are coiled and welded together (see Fig. 1). Today's control of the URW

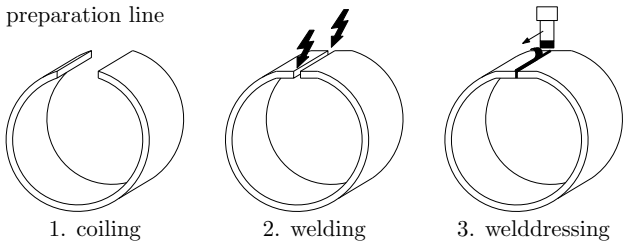

Fig. 1. Overview of the preparation line, which is part of a rim production line.

process and the corresponding theoretical basis are mainly based on practical experience. The quality of a weld is evaluated, often manually, by the size and shape of the upset (the weld nugget). The main part of the controller is a look-up table, which is designed by trial and error.

The quality of a weld is actually determined by the resulting material structure. This structure is heavily dependent on the temperature variations in the material, which makes it thus difficult to define the quality of the weld based on the size and shape of the upset. As a result, material and energy consumption are excessive in minimizing the percentage of loss due to cracking at or just beside the welding seam. Furthermore, setting up and tuning of the process every time a different batch of rims is started often takes much time. Hence, reproducibility is a key aspect in control of the URW process.

[1]Department of Mechanical Engineering, Control Systems Technology group, Technische Universiteit Eindhoven, Eindhoven, The Netherlands. [2]Research and Development Group, Fontijne Grotnes B.V., Vlaardingen, The Netherlands. E-mail: g.j.l.naus@tue.nl, r.meulenberg@fontijnegrotnes.com, m.j.g.v.d.molengraft@tue.nl

Current developments in the field of URW focus on active control of the upset size [1], [2], [3] and reproducibility of the process [4], [5]. However, spot instead of butt resistance welding is emphasized. The spot or upset size is determined and used as a feedback control signal (active control) or as a switching value for stepwise discrete control of the process (semi-active control). Furthermore, research to the influence of heating and cooling ratios on the weld quality of the butt welding process is performed [6]. However, no control research based on the thermodynamical behaviour of the process is present yet.

The contribution of this paper is twofold. Firstly, a relatively simple but accurate simulation model of the process is designed and implemented in Matlab / Simulink. Secondly, a new control strategy for upset resistance butt welding process is developed, targeting at active control of the temperature as well as of the upset size. This enables minimization of set-up times, active control of the weld quality and minimization of material and energy consumption during the process in combination with a high level of reproducibility. A patent is pending for this control strategy.

After an introduction to the weld process and the welding machine (Sec. II), modeling of the weld process is discussed in Sec. III. The model is validated by experiments and used as a basis for controller design. In Sec. IV the design of a new controller enabling active control of the weld quality is presented. Experiments show the proper working of the proposed control strategy.

II. The weld process

The weld process involved is DC upset resistance butt welding. Two sheets of metal, in this case the sheet endings of a coiled rim, are clamped and pushed together with high pressure, called the upset pressure. Under this pressure, elastic deformation of the material takes place. Next, a high magnitude current is directed through the material. Due to the contact resistance in the joint between the sheet endings, the welding seam, heat is generated. This is called the heating phase of the process. The temperature increases till the yield point of the material in the welding seam is reached. The material starts to yield, forming a weld (upset) and an equilibrium is established between the amount of energy supplied and the rate of yielding. This is called the welding phase. If the desired amount of upset is formed, the current is switched off. After a short moment of relaxation of the material, the pressure is released after which the welded rim is removed. The working envelope is determined by specific ranges of the current and the upset pressure for which good

1-4244-0989-6/07/$25.00 ©2007 IEEE.

welds are obtained. To this point, these ranges are determined experimentally.

A. The welding machine

The welding machine used is a test setup with a supply pressure of $100\,\mathrm{bar}$ and a maximum current of $60\,\mathrm{kA}$. A simplified representation of the setup is shown in Fig. 2. The coiled rim is hydraulically clamped by the C-frame with a clamping force F_{cl}. A hydraulic system delivers the force F_h to push the two sheet endings against each other with a pressure p_{up}. The right part of the C-frame is thus moved in horizontal direction x towards the left one. The initial horizontal distance between the clamps equals x_i. Instead of the hydraulic force F_h often the pressure delivered by the hydraulic system p_h is controlled (see Fig. 3). A converter system delivers the current i, which is directed through the material via the electrodes, the clamps of the C-frame. A direct current is used, as this minimizes the amount of sputtering during the process.

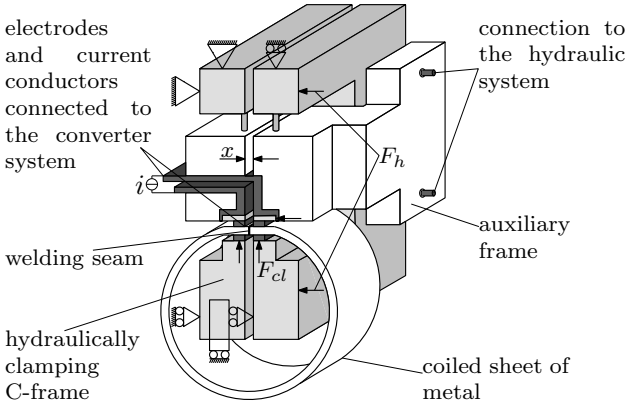

Fig. 2. Overview of the welding machine.

B. Current control system

Currently available welding controllers consists of a closed loop pressure controller tuned by trial and error, and a piecewise open-loop current controller (see Fig. 3). Based on the displacement during the weld process and several time constraints, 5 setpoints for the pressure and the electrical current are prescribed by a look-up table. These setpoints are defined in advance and tuned by trial and error.

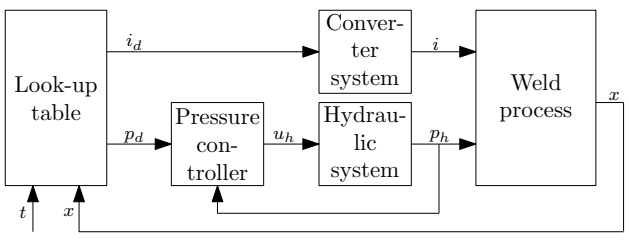

Fig. 3. Common control structure with i_d and p_d the desired current and pressure, u_h the control signal for the hydraulic system, t the time and x the displacement during the weld process.

III. Modeling

A model of the weld process is designed. The model involves the thermodynamics and dynamics of the working area, the hydraulic system and the converter system. The working area encompasses the clamps and the material amid and in between them (see Fig. 4).

A. Thermodynamics of the weld process

Six distinctive parts are determined in the working area (see Fig. 4): the material amid (1), in between (2) and beside the clamps (3), the welding seam (4), the nugget on both sides of the welding seam (5) and the clamps themselves (6). A coarse Finite Element Model (FEM) approach is

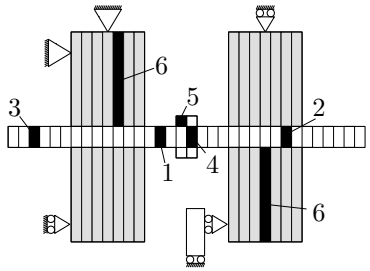

Fig. 4. Front view of the working area. The grey parts represent the clamps, the white parts the clamped material. The degrees of freedom are indicated at the clamps. Six distinctive parts are determined, which are horizontally divided in sections. Per part, one section is filled black and numbered.

adopted, dividing each part horizontally in sections. The temperature of these sections is assumed to be uniform. Hence, calculation of the corresponding balances of energy leads to a set of partial differential equations, describing the thermodynamics of the weld process.

Accordingly, 6 distinctive balances of energy are formulated and assigned to the corresponding sections [7]. The balances of energy incorporate the energy supply by means of heat generation, the loss / supply of energy through conduction, the loss of energy through radiation and the loss / supply of energy through the yielding in the welding seam. The latter one involves the potential or internal energy of the material actually moving from the welding seam to the upset on the welding seam. This is dependent on the speed of deformation or rate of yielding $\dot{x}$. Simulation results show that energy loss through convection is very small with respect to conduction and radiation. Moreover, the air circulation in the working area is negligible. Consequently convection is not taken into account.

The specific temperature of a section j then becomes

$$T_j(t) = \int \frac{\Sigma Q_{s,j}(t) - \Sigma Q_{l,j}(t)}{\rho\, C_p\, dV_j(t)} dt \qquad (1)$$

with $\Sigma Q_{s,j}(t)$ the total supply of energy and $\Sigma Q_{l,j}(t)$ the total loss of energy of a section, ρ the specific mass, C_p the specific heat of the material and $V_j(t)$ the momentary volume of a section.

B. Dynamics of the weld process

The dynamics of the weld process incorporate the dynamical behaviour of the welding machine and of the material in horizontal direction. The hydraulic system is modeled separately. Hence, to this point the welding machine is represented by a moving mass with friction. The elastic and plastic behaviour of the material are represented by a spring respectively a damper. A schematic representation of these dynamics is shown in Fig. 5. The corresponding model is

$$m\ddot{x} = F_h - F_f - k_m(T)x - d_m(T)\dot{x} \tag{2}$$

with x the displacement of the right clamp of the C-frame, m the moving mass of the welding machine, F_h the force delivered by the hydraulic system (see Fig. 2), F_f the friction force and k_m and d_m temperature dependent material parameters.

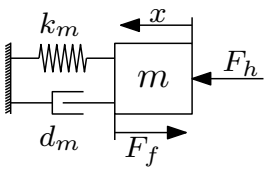

Fig. 5. Dynamics of the welding machine and the material, with F_h the force delivered by the hydraulic system and x the displacement of the right clamp (see Fig. 2).

Measurements show that the viscous friction is negligible and the static friction is very small compared to the Coulomb friction. Hence, the following model for the friction force F_f is adopted

$$F_f \quad = \quad \begin{cases} f^+ & \text{for } \dot{x} > 0 \\ f^- & \text{for } \dot{x} < 0 \\ 0 & \text{for } \dot{x} = 0 \end{cases} \tag{3}$$

with f^+ and f^- the actually measured friction forces in positive and negative moving direction respectively. The clamping forces F_{cl} (see Fig. 2) and the corresponding friction forces between the clamps and the clamped material are that high, the corresponding relative displacement may be assumed negligible.

The dynamical behaviour of the material is elastic during the heating phase and plastic during the welding phase. Elastic behaviour is dominated by the stiffness k_m of the material, while temperature dependent damping d_m dominates the plastic behaviour. Due to the thinness of the metal, the actual horizontal elasticity of the material is smaller than the Young's modulus. This value thus has to be defined experimentally for each new set of coils. The temperature dependent damping during the welding phase $d_m^w(T)$ is defined using a linear interpolation between the yield temperature T_y and the melt temperature T_m of the material

$$d_m^w(T) = d_{m,T_y}\left(1 - \frac{T(t) - T_y}{T_m - T_y}\right) \tag{4}$$

with d_{m,T_y} the initial damping at $T(t) = T_y$, which has to be defined experimentally as well. The yield point actually is a transition region in which the elastic behaviour gradually changes to plastic behaviour. Hence for simulation purposes more extended modeling, taking into account this transition is performed as well. For control purposes however, this is not of importance.

C. Validation of the thermodynamics and dynamics modeling

To validate the modeling of the weld process, simulation results are compared to experimental measurements. Variation of the process parameters, i.e. magnitude of the input pressure p_h and the input current i, size of the coiled rim's cross section and material type, assures validation over the complete envelope of working conditions. The displacement x is considered as output (see Fig. 3).

In Fig. 6 the results for varying magnitude of electrical current i are shown. These results show good correspondence between the modeled and measured displacements.

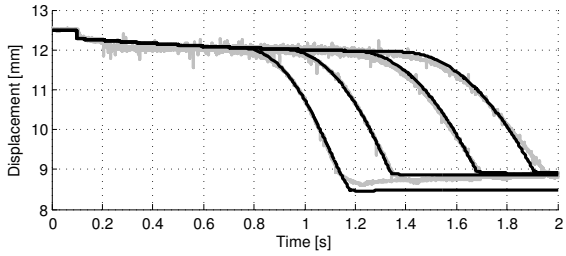

Fig. 6. Experimental validation measurements (the light grey curves) compared to simulation results (the black curves on top) for varying magnitudes of the electrical current. With an initial distance between the clamps of $x_i = 12.5\,\text{mm}$, the hydraulic force F_h is applied (at $0.1\,\text{s}$) to remove irregularities and to achieve good contact in the welding seam. The current is switched on and the material is heated. During this heating phase the material behaviour is elastic. When the yield temperature T_y is reached, this behaviour becomes plastic and the material starts to yield until the electrical current is switched off. F_h is released a moment later.

Using thermo-couples and an infrared camera, an approximation of the actual temperature in the welding seam is made to validate the temperature calculation (see Fig. 7). The results show that the modeled progress of the temperature compares well to the measurements till the yield point is reached (the heating phase). For final control of the process,

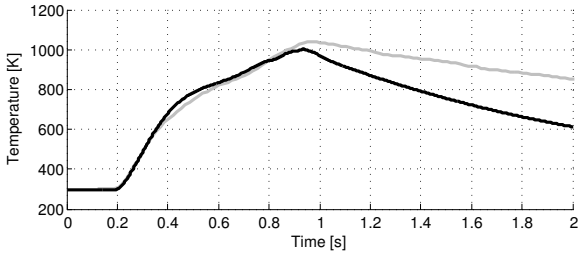

Fig. 7. Simulation results (the black curve on top) compared to experimental measurements (the light grey curve) using an infrared camera. The temperature of the welding seam is shown.

only the relative temperature progress with respect to the yield point temperature during this heating phase is of

importance. The correctness of the rest of the temperature calculation is of minor importance to this point.

Based on the results for a complete envelope of working conditions, it is concluded that the presented model for the weld process is suitable for use in model-based controller design.

D. Converter system

The electrical DC current is delivered by a combined inverter and transformer system, the converter system. An output current of 0 to 60 kA is generated corresponding to an input voltage of 0.0 to 1.0 V. The built-in current controller has a bandwidth bw_c of approximately 100 Hz, which is much higher than the desired overall control bandwidth. Consequently the converter system is modeled as a 2^{nd}-order filter with a cut-off frequency at bw_c.

E. Hydraulic system

The hydraulic system of the welding machine consists of an electric hydraulic servo-valve in combination with a symmetric hydraulic cylinder. Based on frequency response measurements, a linear model is designed (see [8]). The resulting model encompasses the linear transfer from u_h to p_h (see Fig. 3).

IV. Controller design

Based on the modeling of the weld system, a model-based controller is developed. The resulting controller is a piecewise linear MIMO feedback tracking controller. In Fig. 8(a) the implementation of the proposed control strategy is shown. As it is relatively difficult and costly to measure the welding seam temperature T_{ws} directly, the controller, i.e. the *Weld system*, includes an online calculation of the welding seam temperature T_{ws} (see Fig. 8(b)). In this way the proposed strategy can be implemented easily on the present machines. The temperature calculation is derived from the modeling of the thermodynamics of the process.

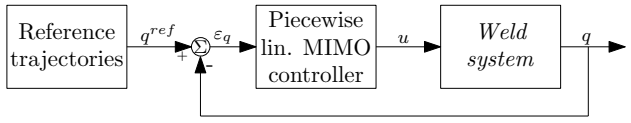

(a) controller implementation

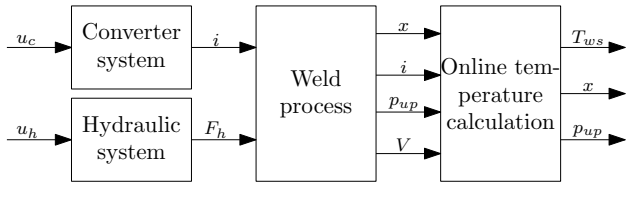

(b) *Weld system*

Fig. 8. (a): The proposed controller structure with $q = (T_{ws},\, p_{up},\, x)^T$ the control inputs and $u = (u_c,\, u_h)^T$ the control outputs. ε_q represents the error between the reference trajectories q^{ref} and the actual process variables q. (b): Schematic representation of the *Weld system* of Fig. 8(a) in more detail (see the Nomenclature for explanation of the symbols).

A. Linearisation

Classical linear control theory using frequency-based loop shaping techniques is used to tune the controller. For this purpose, the model of the weld process is linearized. Fig. 9 shows simulation results of the nonlinear model and a couple of linear models. A clear distinction can be made between the heating phase (0.1 till 0.8 s) and the welding phase (0.8 till 1.3 s). The phases are separated by attenuation of the yield temperature, called the yield point. During the heating phase, constant heating and no deformation of the material are assumed, while constant deformation and constant temperature are assumed in the welding phase. The

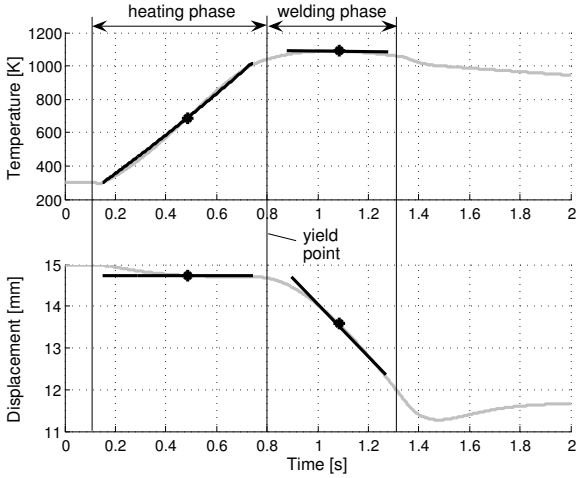

Fig. 9. Simulation results of the nonlinear model (grey curves) and several linear models (black curves). The black stars indicate the used linearisation points.

transition from the heating phase to the welding phase in fact encompasses a region rather than a point (see the start of the welding phase in Fig. 9). Hence, stability of the total welding phase has to be verified afterwards.

B. Sequential loop closing and loop shaping

From linearisation two linear models describing the heating and the welding phase, H^h respectively H^w, follow. This leads to a piecewise linear controller C^i, with $i = h, w$ the index for the heating respectively the welding phase.

With H^i the *Weld system* and C^i the controller, the closed-loop system becomes

$$q = H^i\, u, \qquad \text{with } H^i(3 \times 2) \tag{5}$$

$$u = C^i\, \varepsilon_q, \qquad \text{with } C^i(2 \times 3) \tag{6}$$

with $q = (T_{ws}, p, x)^T$, $u = (u_c, u_h)^T$, $\varepsilon_q = (\varepsilon_{T_{ws}}, \varepsilon_p, \varepsilon_x)^T$ (see Fig. 8).

Modeling and experimental validation show that the magnitude of H^h_{12} and H^h_{21} are negligible compared to H^h_{11} and H^h_{22}. Furthermore, only the temperature and pressure are controlled during the heating phase. Consequently, the system is decoupled in the heating phase and two SISO control loops incorporating C^h_{11} and C^h_{22} result. During the

welding phase only the displacement or deformation x is controlled. Hence, a MISO system with u the inputs and $q = x$ the output, remains. This leads to a SIMO controller C^w.

Standard loop shaping techniques can be applied to tune C^h. In the welding phase however, the system is not decoupled and the two (closed) loops are influencing each other. By applying Sequential Loop Closing (SLC), this effect is taken into account [9]. I.e. if C^w_{13} is designed based on H^w_{31}, the transfer function H^w_{32} 'felt' by C^w_{23} changes to

$$H^w_{32,slc} = \frac{H^w_{32}}{1 + H^w_{31} C^w_{13}} \tag{7}$$

Analogously, after implementation of C^w_{23}, the transfer function H^w_{31} 'felt' by C^w_{13} changes to

$$H^w_{31,slc} = \frac{H^w_{31}}{1 + H^w_{32} C^w_{23}} \tag{8}$$

SLC comprises controller design based on these perturbed transfer functions (Eq. 7 or 8), thus enabling stable MIMO controller design using traditional loop shaping techniques. The first part of the controller is designed based on the original system transfer functions H^w, whereas the second controller then is designed based on the perturbed transfer functions H^w_{slc}.

No general rules are defined in which order the loops should be closed. In this case, the modeling of H^w_{31} is less accurate than H^w_{32}. Consequently C^w_{23} is designed first, based on H^w_{32}. After that, C^w_{13} is designed based on $H^w_{31,slc}$ (see Fig. 10). Using standard PID actions and filters, all controller parts are designed. In Table I the resulting controller bandwidths, which are defined as the 0-dB crossing of the corresponding open-loop transfer functions, are presented.

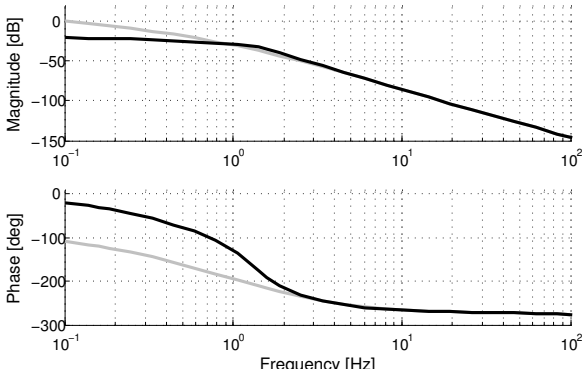

Fig. 10. The grey curve shows the original transfer function H^w_{31}, the black curve shows the transfer function $H^w_{31,slc}$ actually 'felt' by C^w_{13} after application of C^w_{23}.

C. Switching control

A switching strategy for the transition from the heating to the welding phase connecting the two successive controllers C^h and C^w, is needed. Reaching the yield point determines the start of the transition of elastic to plastic material behaviour. The transition is described by a decrease of k_m and an increase of d_m and involves a change in control objectives. The pressure and the temperature of the welding seam are controlled in the heating phase, while the displacement is controlled during the welding phase.

TABLE I
RESULTING CONTROLLER BANDWIDTHS.

Controller part	Bandwidth in [Hz]
C^h_{11}	10
C^h_{22}	65
C^w_{13}	4
C^w_{23}	4

An often used method is the gradual transition between the two point design controllers via linear interpolation. A varying controller gain ζ is defined

$$\zeta = \frac{t - t_1}{t_s} \tag{9}$$

with t_1 the starting time of the switching controller and t_s the total switching time. The starting time is taken equal to the start of the transition region, the yield point. The linear interpolation leads to the following control output u during switching (see Fig. 11).

$$u = \begin{pmatrix} (1-\zeta)C^h_{11} & 0 & \zeta\, C^w_{13} \\ 0 & (1-\zeta)C^h_{22} & \zeta\, C^w_{23} \end{pmatrix} \varepsilon_q \tag{10}$$

with u and ε_q as in Eq. 6.

A thorough stability analysis is the subject of future work. The LPV synthesis probably provides a good framework for this analysis. To this point it is assumed that the system remains stable if the transition from the stable closed loop system T^h to the stable closed loop system T^w is gradual. This means that t_s is limited with a minimum, which is determined experimentally.

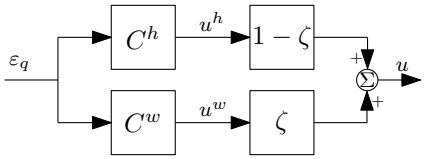

Fig. 11. Schematic representation of the control structure during switching.

D. Reference trajectories

As a feedback tracking controller is present now, reference trajectories for the temperature of the welding seam T_{ws}, the output pressure of the hydraulic system p_h and the displacement x during the weld process can be designed. In this way the desired weld process dynamics and weld quality can be defined.

During the heating phase, the pressure and temperature are controlled, whereas during the welding phase the displacement is controlled. The design of the trajectories is based on (1) material dependent settings, e.g. the yield temperature, (2) setup dependent settings, e.g. the environmental temperature and the material's cross section size determining the required pressure and (3) user-defined settings, e.g. the amount of

upset and the time the process should take. The grey curves in Fig. 12) show an example of the reference trajectories.

E. Simulation and experimental results

The resulting controller is designed in Matlab/Simulink. The controller is loaded onto a dSpace DS1103 PPC controller board, establishing the connection to the welding machine. In Fig. 12 the results of a weld process after implementation of the controller are shown.

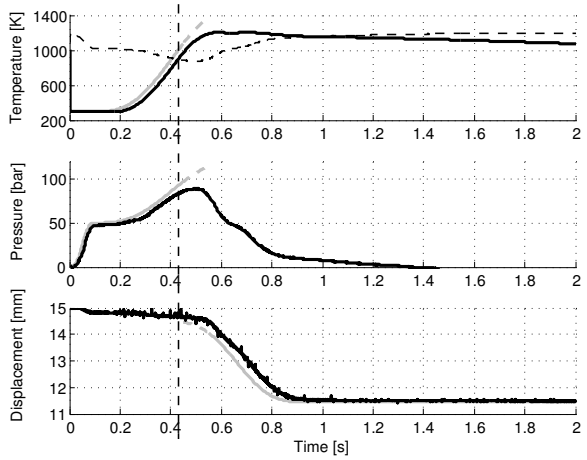

Fig. 12. Experimental results of the weld process after implementation of the new controller. The grey curves show the reference trajectories, the black curves show the online calculated temperature, the measured pressure and the measured displacement. The dashed black curve in the upper plot shows the online calculation of the yield temperature, the line indicates the yield point.

Experimental results show that the total weld time and the reproducibility of the process are at the required level, comparable to results of the current control system. First results also indicate a significant decrease of energy consumption as well as of the set-up times. Conclusions about material consumption and percentage of loss with respect to the current system can only be drawn after implementation on a commercially available welding machine.

V. Conclusions

A relatively simple but accurate simulation model is designed. Based on this model a new controller for the upset resistance butt welding process is designed, enabling active control of the weld quality. As a result, energy consumption and set-up times are decreased significantly.

VI. Recommendations and future work

Implementation and testing of the control strategy on a commercially available welding machine have to show the actual benefits regarding material and energy consumption, the percentage of loss and the set-up times. Preliminary test results show a significant reduction in upset. Furthermore, a thorough stability analysis of the adopted switching strategy has to be performed.

References

[1] Bosch Rexroth AG.; *Ultrasonic In-Process Adaptive Resistance Welding QA System*, (http://www.boschrexroth.com), Electric Drives and Controls Division, 2002.

[2] Medar; *Thermal Force Feedback (TFF®) System*, (http://www.medar.com), Welding Technology Corporation, May 2003.

[3] H.A. Schlatter AG.; *Schlatter Weld Program*, http://www.schlatter.ch, Schlatter Holding AG, 2006.

[4] Automation International Inc.; *the Assurance Program*, (http://www.automation-intl.com), Automated Welding and Metalworking Machines, 2006.

[5] New Southern Resistance Welding (NSRW); *Weldcomputer Adaptive Control*, (http://www.nsrw.com), Pelham, Alabama, 2004.

[6] Netherlands Institute for Metal Research (NIMR); *Joining Technologies*, (http://www.nimr.nl), Joining technologies under coordination of Prof. Ian Richardson, Delft, the Netherlands, 2006.

[7] Bejan A.; *Heat Transfer*, ISBN: 0-471-59503-9, John Wiley & Sons, 1993.

[8] Viersma, T.J.; *Analysis, Synthesis and Design of Hydraulic Servosystems and Pipelines*, ISBN: 0-444-41869-5, Elsevier, revised edition, 1990.

[9] Bryant, G.F. and Yeung, L.F.; *Multivariable Control System Design Techniques: Dominance and Direct Methods*, ISBN: 0-471-95866-2, John Wiley & Sons, 1996.

Nomenclature

C_p	specific heat	$(J\,kg^{-1}K^{-1})$
d_m	material specific damping	$(Ns\,m^{-1})$
$f^{\pm}$	$\pm$ Coulomb friction force	(N)
F_{cl}	vertical clamping force	(N)
F_f	friction force	(N)
F_h	hydraulic system output force	(N)
i	direct electrical current	(A)
k_m	material specific stiffness	(Nm)
p_h	hydraulic system output pressure	(bar)
p_{up}	pressure in the welding seam	(bar)
q	vector with process variables	
q^{ref}	reference trajectories for q	
Q	energy	(J)
t_s	switching time	(s)
t_1	starting time of the switching	(s)
T	temperature	(K)
T_m	melt temperature	(K)
T_{ws}	welding seam temperature	(K)
u	vector with control signals	
u_c	converter system control signal	(V)
u_h	hydraulic system control signal	(A)
T_y	yield temperature	(K)
V	volume	(m^3)
V	voltage	(V)
x	horizontal displacement	(m)

Greek letters

ε_q	difference between q and q^{ref}	
ρ	specific mass	$(kg\,m^{-3})$

Super and subscripts

$_h$	heating phase
$_i$	initialisation value
$_j$	section index number
$_l$	loss
$_s$	supply
$_w$	welding phase